

Comparative Study on Efficiency of Mirror Retroreflectors

João Pedro Cruz^(✉) and Alexander Plakhov

Universidade de Aveiro, Aveiro, Portugal
{pedrocruz,plakhov}@ua.pt

Abstract. Here we study retroreflectors based on specular reflections. Two kinds of asymptotically perfect specular retroreflectors in two dimensions, Notched angle and Tube, are known at present. We conduct comparative study of their efficiency, assuming that the reflection coefficient is slightly less than 1. We also compare their efficiency with the one of the retroreflector Square corner (the 2D analogue of the well-known and widely used Cube corner). The study is partly analytic and partly uses numerical simulations. We conclude that the retro-reflectivity ratio of Notched angle is normally much greater than those of Tube and the Square corner. Additionally, simple Notched angle shapes are constructed, whose efficiency is significantly higher than that of the Square corner.

Keywords: Retroreflectors · Geometric optics · Shape optimization · Billiards

Mathematics subject classifications: 49Q10, 49M25, 78A05.

1 Introduction

A retroreflector is an optical device that reverts the direction of incident beams of light [9]. In the framework of geometric optics one deals with light rays that propagate along straight lines (in a homogeneous space) or curves. The retroreflector is called to be *perfect*, if each incident light ray, as a result of interaction with the device, changes its direction to the opposite (such rays are called *retro-reflecting*).

Retroreflectors are widely used in economy, for example in road safety and space exploration. Most retroreflectors used in practice are not perfect: only a part of incident light rays are retro-reflected. The most used types of retroreflectors are called *cube corner* and *cat's eye* (see Fig. 1). The former one is based on reflection from three mutually perpendicular planes, and the latter one, on refraction in a lens (and possibly also reflection). Both are not perfect.

A well-known example of perfect retroreflector is *Eaton lens*, a transparent ball with the varying refractive index [2–4, 8]. More precisely, the refractive index at a point of the ball equals $n(r) = \sqrt{2R/r - 1}$, where R denotes the radius of the ball and r the distance from the point to the ball center. That is, the index equals 1 at the boundary of the ball and goes to infinity when the point approaches the ball center. An incident light ray passes through the ball and then goes back in the direction opposite to the original one (see Fig. 2).

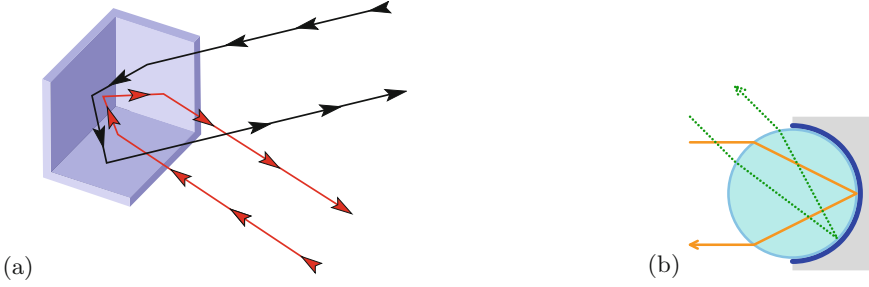


Fig. 1. The retroreflectors (a) Cube corner and (b) Cat's eye.

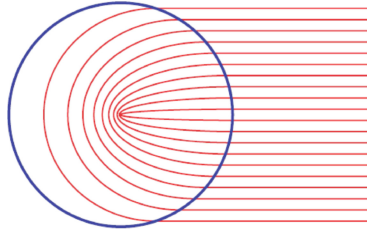


Fig. 2. Eaton lens.

However, design of media with varying refractive index is not an easy task. It seems to be much easier from technical viewpoint to design retroreflectors based solely on mirror reflections, or billiard retroreflectors. Thus, one comes to the problem of creating a perfect billiard retroreflector.

This problem is not solved until now. It is even not known if such retroreflectors really exist. What we know, however, is that there exist *asymptotically perfect* families of retroreflectors [1, 5, 7]. For arbitrarily small $\varepsilon > 0$, one can choose a retroreflector in such a family so that the portion of light rays reflected from it in wrong directions is smaller than ε . At present, 2D asymptotically perfect retroreflectors are studied in some detail, and almost nothing is known about 3D ones. Notice that 2-dimensional devices may be of interest for practice, especially if the light is supposed to propagate in a single plane. For instance, one can imagine applications in road engineering, when the retroreflectors are placed on the height corresponding to the level of the driver's eyes.

In this paper we concentrate on 2-dimensional asymptotically perfect families of retroreflectors. By a retroreflector we mean a bounded domain B with a marked part of the boundary. The marked part is a line segment (the dashed line in Fig. 3); it is called the *inlet* of the retroreflector. The retroreflector lies on one side of the dashed line, and its boundary is a piecewise smooth curve with finite length.

The propagation of light is represented by the billiard in B . A light ray comes through the inlet, makes several reflections from the boundary ∂B , and finally leaves B through the inlet. The ray is retro-reflected, if the direction of coming in is opposite to the direction of going away ($\varphi = \varphi^+$ in Fig. 3). We

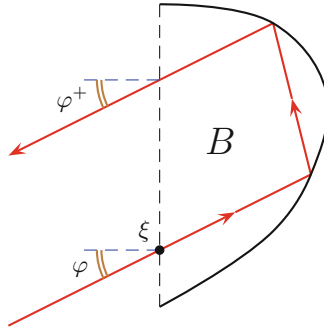


Fig. 3. Motion of light in a retroreflector.

parameterize the inlet by $\xi \in [0, 1]$; each incident ray is naturally labeled by the angle of incidence φ varying from $-\varphi/2$ to $\varphi/2$ and by the point ξ where the ray intersects the inlet.

For a retroreflector B , the *retro-reflectivity ratio* $r(B)$ is the portion of the incident light rays that are retro-reflected by the device. The ratio varies between 0 (no retro-reflection at all) and 1 (perfect retro-reflection). The amount of incoming light is counted according to the natural billiard measure $d\mu(\varphi, \xi) = \frac{1}{2} \cos \varphi d\varphi d\xi$ defined on $[-\pi/2, \pi/2] \times [0, 1]$. It is a probability measure, that is, $\mu([-\pi/2, \pi/2] \times [0, 1]) = 1$.

It is instructive to calculate the retro-reflectivity ratio of the *square corner*, the 2-dimensional analogue of cube corner (see Fig. 4). Assume that the sides of the corner are perfectly reflecting. Any light ray that makes 2 reflections from the corner reverts its direction, and a ray that makes only 1 reflection goes away in a wrong direction. A simple geometrical analysis allows one to calculate the portion of rays that make double reflections (and therefore are retro-reflected); see Fig. 4 for a graphical illustration. We find that for a fixed φ the portion of retro-reflected rays equals

$$R_{cq}(\varphi) = \begin{cases} 1 - |\tan \varphi|, & \text{if } |\varphi| < \pi/4; \\ 0, & \text{if } |\varphi| \geq \pi/4 \end{cases}$$

(and hence the portion of wrongly reflected rays is $1 - R_{cq}(\varphi)$). Therefore the retro-reflectivity ratio of the square corner equals

$$r_{sq} = \int_{-\pi/2}^{\pi/2} R_{cq}(\varphi) \frac{1}{2} \cos \varphi d\varphi = \int_0^{\pi/4} (\cos \varphi - \sin \varphi) d\varphi = \sqrt{2} - 1 \approx 0.414.$$

Note that this analysis is not applicable to the second most popular type of retroreflectors: cat's eye. The point is that generally the direction of reversed light rays in cat's eyes does not precisely coincide with the direction of incidence, but is slightly deviated. Thus the formal calculation of the retro-reflectivity ratio would give zero.

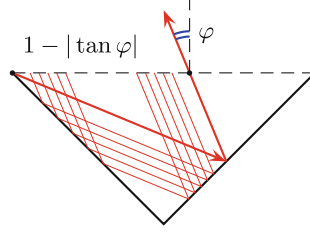


Fig. 4. Reflection of light in a square corner.

At present two asymptotically perfect retroreflectors, *Tube* and *Notched angle*, are known. They are obtained by modifying a rectangle and an isosceles triangle, respectively. Notice that both a rectangle with small $q = (\text{height})/(\text{width})$ and an isosceles triangle with small $q = (\text{base})/(\text{height})$ can serve as retroreflectors (see Fig. 5), and their retro-reflectivity ratios go to $1/2$ as $q \rightarrow 0$ (see [6], Chap. 9).

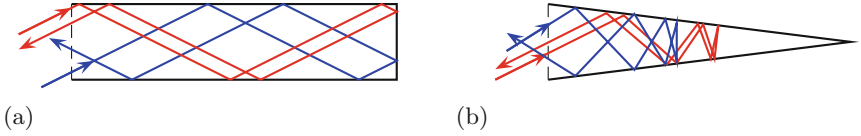


Fig. 5. (a) Rectangle-shaped and (b) triangle-shaped retroreflectors. In both cases the retro-reflected ray is shown red, and the wrongly reflected ray is shown blue.

Tube is obtained by removing small periodically located segments parallel to the inlet from a rectangle (see Fig. 6). More precisely, a Tube $B(n, d, \varepsilon)$ is the rectangle $[0, (n+1)d] \times [0, 1]$ with the segments $\{di\} \times [0, \varepsilon]$ and $\{di\} \times [1-\varepsilon, 1]$, $i = 1, \dots, n$ removed; that is,

$$B(n, d, \varepsilon) = [0, (n+1)d] \times [0, 1] \setminus \bigcup_{i=1}^n (\{di\} \times ([0, \varepsilon] \cup [1-\varepsilon, 1])).$$

Here the inlet is $\{0\} \times [0, 1]$. Thus, the retroreflector Tube depends on three parameters: n , d , and ε . It is proved in [1, 5] that for a certain family of retroreflectors $B(n, d, \varepsilon)$ with $\varepsilon \rightarrow 0$, $n = n(\varepsilon) \rightarrow \infty$, and with d fixed, the retro-reflectivity ratio $r(B(n(\varepsilon), d, \varepsilon))$ goes to 1 as $\varepsilon \rightarrow 0$.

Notched angle is obtained by replacing the lateral sides of the rectangle with a broken line whose segments are parallel and perpendicular to the inlet (see Fig. 7). More precisely, take positive δ , α , β , consider the broken line composed of alternating horizontal and vertical segments inscribed in the angle $x \tan \alpha \leq y \leq x \tan(\alpha + \beta)$ and situated between the vertical lines $x = \delta$ and $x = 1$. Further consider another broken line symmetric to the original one with respect to the x -axis. The initial endpoints of the former and latter lines are $(1, \tan \alpha)$ and $(1, -\tan \alpha)$, respectively.

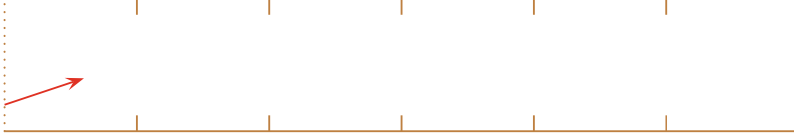


Fig. 6. The Tube $B(5, 1, 0.12)$, with the number of segments $n = 5$, horizontal distance between the segments $d = 1$, and the length of each segment $\varepsilon = 0.12$.

The Notched angle $B(\alpha, \beta, \delta)$ is bounded by these broken lines and by the vertical lines $x = \delta$ and $x = 1$. The inlet is the vertical segment $\{1\} \times [-\tan \alpha, \tan \alpha]$. Thus, the retroreflector Notched angle depends on three parameters: α , β , and δ . It is proved in [5] that for a certain family of retroreflectors $B(\alpha, \beta, \delta)$ with $\delta = \delta(\alpha) \xrightarrow{\alpha \rightarrow 0} 0$, $\beta = \beta(\alpha)$, $\beta/\alpha \xrightarrow{\alpha \rightarrow 0} 0$ the retro-reflectivity ratio $r(B(\alpha, \beta(\alpha), \delta(\alpha)))$ goes to 1 as $\alpha \rightarrow 0$.

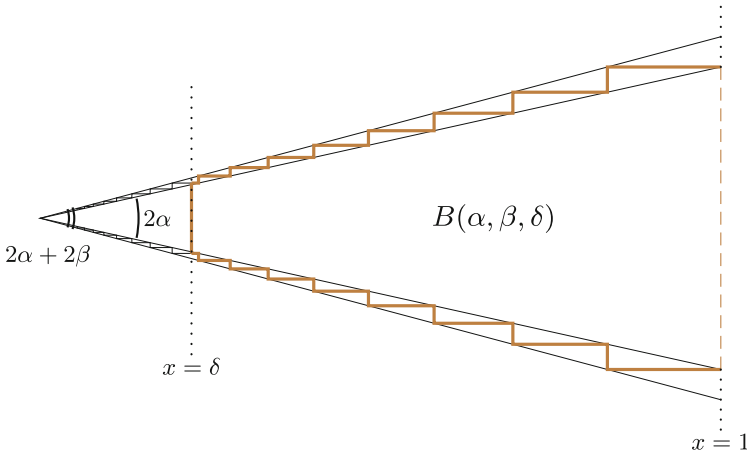


Fig. 7. Notched angle.

Our aim in this paper is to evaluate and compare the efficiency of these retroreflectors. It is supposed that a part of the light is lost after each reflection: a portion k of the light is reflected according to the billiard law, and the portion $1 - k$ is absorbed by the device or scattered. Here $0 < k < 1$. We are going to evaluate the three parameters (a , b , ε in the former case and α , β , δ in the latter case) that provide the maximal, or nearly maximal, retro-reflectivity ratio. Obviously, when k goes to 1 (full reflection), the maximum retro-reflectivity ratio goes to 1 in both cases. We will see, as a result of our study, that for each k the retroreflector Notched angle is much more efficient than the Tube.

Another question we address here concerns creating a reflecting curve with relatively simple shape and with the retro-reflectivity ratio significantly greater than that of the square corner. We will see that such shapes do exist.

Finding a 3D analogue of the Tube and (especially) the Notched angle are challenging tasks for the future.

2 Notched Angle

2.1 Analytical Study

One of the advantages of Notched angle is that its efficiency can be evaluated analytically. Here we provide analytical derivation of the retro-reflectivity ratio $r(\alpha, k)$ in the limit when $\beta \rightarrow 0$, $\delta \rightarrow 0$. It can be made rigorous with using methods from [5]. However, here we limit ourselves by numerical verification of our heuristics.

First consider two flows of particles with the angles of incidence φ and $-\varphi$, with $0 < \varphi < \alpha$. Fix an indentation (the line ABC in Fig. 8) of our angle and consider the part of the flow incident on it with the angle φ . The segment AB is vertical and BC is horizontal. By unfolding the right triangle ABC one obtains the isosceles triangle AEC . The point F on the side AC is chosen so that the line EF forms the angle φ with EC .

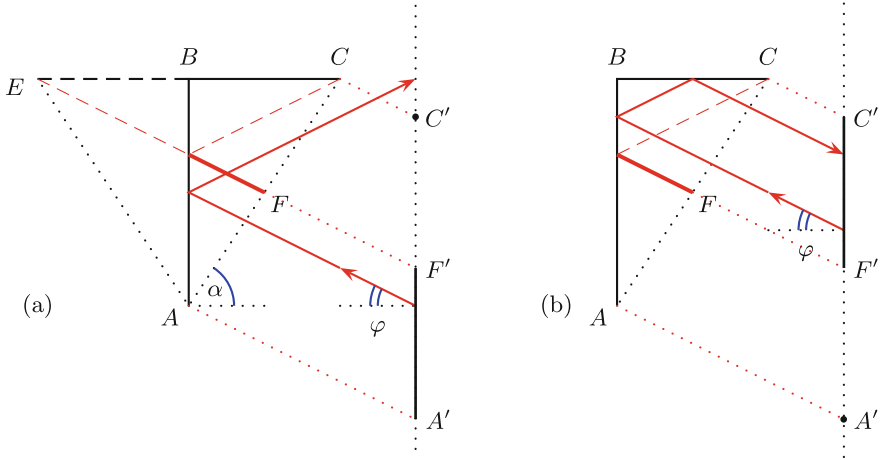


Fig. 8. Particles reflected from an indentation when $|\varphi| \leq \alpha$. (a) A wrongly reflected particle. (b) A retro-reflected particle.

If a particle comes through the segment AF , it makes a reflection and is reflected in a wrong direction (see Fig. 8(a)). If it comes through FC , it makes two reflections and is retro-reflected (see Fig. 8(b)).

The triangle AEF has the angles $\pi - 2\alpha$, $\alpha - \varphi$, $\alpha + \varphi$, respectively. The triangle CEF has the angles α , φ , $\pi - \alpha - \varphi$, respectively. Applying the sine law to these triangles, after a simple trigonometry one obtains

$$\frac{|FC|}{|AC|} = \frac{2 \tan \varphi}{\tan \alpha + \tan \varphi}. \quad (1)$$

Consider a vertical line (for example, the inlet of the notched angle). The particles incident on the given indentation with the angle of incidence φ intersect this line at points of a certain segment (the segment $A'C'$ in Fig. 8 (a), (b)). Using again the sine law, one easily finds the length of the segment,

$$|A'C'| = |AC| \frac{\sin(\alpha + \varphi)}{\cos \varphi}.$$

The segment $F'C'$ (see Fig. 8 (b)) corresponds to the retro-reflected particles. Using (1), one easily finds its length,

$$|F'C'| = |AC| \cdot 2 \tan \varphi \cos \alpha.$$

On the other hand, all the particles with the angle of incidence $-\varphi$ (not shown in the figure) are reflected from the indentation in a wrong direction. The length of the corresponding vertical segment equals

$$|AC| \frac{\sin(\alpha - \varphi)}{\cos \varphi}.$$

Thus, the total length of the segments corresponding to the two flows equals

$$|AC| \frac{\sin(\alpha + \varphi)}{\cos \varphi} + |AC| \frac{\sin(\alpha - \varphi)}{\cos \varphi} = |AC| \cdot 2 \sin \alpha,$$

and only one segment with the length $|AC| \cdot 2 \tan \varphi \cos \alpha$ corresponds to the retro-reflected particles. That is, the portion of retro-reflected particles equals

$$\frac{|AC| \cdot 2 \tan \varphi \cos \alpha}{|AC| \cdot 2 \sin \alpha} = \frac{\tan \varphi}{\tan \alpha}.$$

Note that it does not depend on the specific indentation. Integrating this value over $\varphi \in [-\alpha, \alpha]$ and taking into account the absorption, one finds the portion (among all incident particles) of retro-reflected particles with the angles $|\varphi| \leq \alpha$,

$$r_1(\alpha, k) = k^2 \int_{-\alpha}^{\alpha} \frac{\tan \varphi}{\tan \alpha} \frac{1}{2} \cos \varphi d\varphi = k^2 \frac{\cos \alpha (1 - \cos \alpha)}{\sin \alpha}.$$

Let now $\varphi > \alpha$. Consider the flow of particles incident on a fixed indentation (the line ABC in Fig. 9) with the angle of incidence φ . Let the triangle EBC be symmetric to the triangle ABC with respect to the line BC . Take the point F on AC so that EF forms the angle φ with BC . If the particle comes through the segment AF , it makes two reflections and goes back in the opposite direction. If it comes through FC then after a single reflection it continues moving forward.

The triangle AEF has the angles $\pi/2 - \alpha$, $\pi/2 - \varphi$, $\alpha + \varphi$, respectively. The triangle CEF has the angles 2α , $\varphi - \alpha$, $\pi - \alpha - \varphi$, respectively. Applying the sine rule to these triangles, one comes to the relation

$$\frac{|FC|}{|AC|} = \frac{\tan \varphi - \tan \alpha}{\tan \varphi + \tan \alpha} =: \lambda_{\alpha}(\varphi).$$

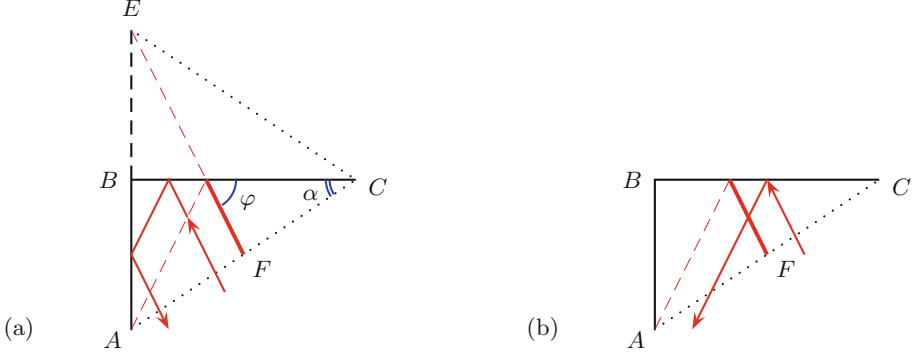


Fig. 9. Particles reflected from an indentation when $\varphi > \alpha$. (a) A retro-reflected particle. (b) A wrongly reflected particle.

This ratio is the portion of the flow that continues moving forward after being reflected in the indentation. It does not depend on the specific indentation.

The process can be described as follows. The part $1 - \lambda$ (where $\lambda = \lambda_\alpha(\varphi)$) of the flow is retro-reflected by the first indentation (after hitting it two times). Thus, the retro-reflected part of the flow is $k^2(1 - \lambda)$. Notice that the first indentation may be different for different particles.

The part of the flow retro-reflected by the second indentation is $\lambda(1 - \lambda)$. The corresponding particles make one reflection while moving forward, two reflections in the indentation, and one reflection on the way back — 4 reflections in the total. The retro-reflected part of the flow is $k^4\lambda(1 - \lambda)$.

Continuing this process, one obtains the sequence $k^{2m+2}\lambda^m(1 - \lambda)$, $m = 0, 1, 2, \dots$, the sum of its terms being the portion of retro-reflected particles,

$$k^2(1 - \lambda)[1 + k^2\lambda + k^4\lambda^2 + \dots] = \frac{k^2(1 - \lambda)}{1 - k^2\lambda}.$$

Here $\lambda = \lambda_\alpha(\varphi)$. Notice that this portion is related to the flow with the angle of incidence φ . The portion of retro-reflected particles corresponding to all angles $\varphi > \alpha$ is obtained by integration,

$$r_2(\alpha, k) = \int_{\alpha}^{\pi/2} \frac{k^2(1 - \lambda_\alpha(\varphi))}{1 - k^2\lambda_\alpha(\varphi)} \cos \varphi d\varphi = \int_{\tan \alpha}^{\infty} \frac{2k^2}{\frac{t}{\tan \alpha}(1 - k^2) + (1 + k^2)} \frac{dt}{(1 + t^2)^{3/2}}.$$

Thus, the retro-reflectivity ratio equals

$$\begin{aligned} r(\alpha, k) &= r_1(\alpha, k) + r_2(\alpha, k) \\ &= k^2 \frac{\cos \alpha(1 - \cos \alpha)}{\sin \alpha} + \int_{\tan \alpha}^{\infty} \frac{2k^2}{\frac{t}{\tan \alpha}(1 - k^2) + (1 + k^2)} \frac{dt}{(1 + t^2)^{3/2}}. \end{aligned} \quad (2)$$

The graphs of $r(\alpha, k)$ as functions of α for several values of k are shown in Fig. 10. The optimum angle $\alpha_{\max} = \alpha_{\max}(k)$ is indicated by a dot on each curve. The values of the angles α_{\max} and the corresponding retro-reflectivity ratios are given in the table below.

| | | | | |
|-----------------------|-------|-------|-------|-------|
| k | 0.5 | 0.8 | 0.9 | 0.99 |
| α_{\max} | 0.445 | 0.356 | 0.287 | 0.117 |
| $r(\alpha_{\max}, k)$ | 0.146 | 0.421 | 0.582 | 0.864 |

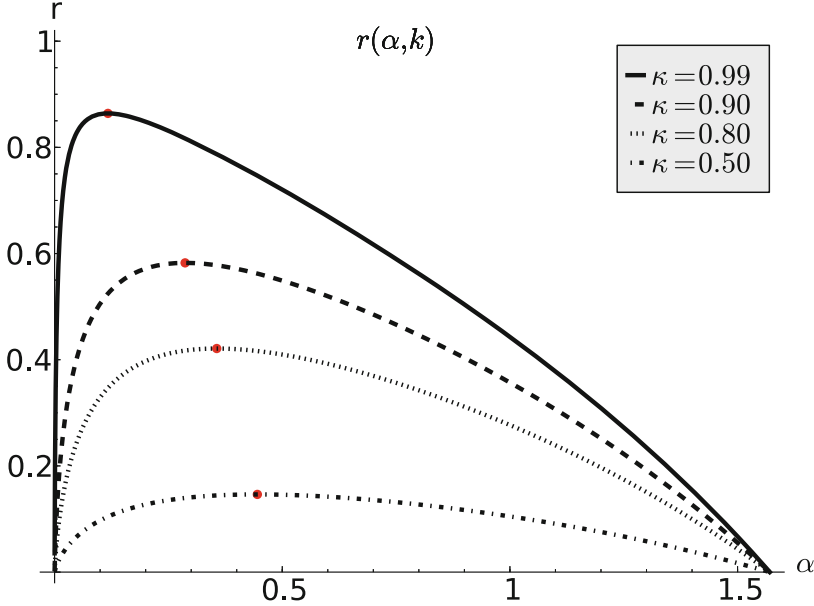


Fig. 10. Retro-reflectivity ratio $r(\alpha, k)$ of Notched angle for several values of k .

2.2 Numerical Simulation

The number of light beams coming through the inlet was chosen to be 1000 in all experiments. If \bar{r} is the estimate of the retro-reflectivity ratio in a simulation, then the standard deviation of the estimate is less than 2 %, as can be seen from the formula for the deviation of Normal distribution $\sqrt{\bar{r}(1 - \bar{r})/1000}$ for $\bar{r} \in [0, 1]$.

In the case of positive β and δ there are no analytic formulas, so one needs to proceed to numerical simulation. First we verify theoretical results for the limiting case $\beta \rightarrow 0$, $\delta \rightarrow 0$. To that end, we calculate the retro-reflectivity ratio $r(\alpha_{\max}, \beta, \beta, k)$ for the fixed values $k = 0.9$ and $k = 0.99$ and the corresponding optimal values $\alpha_{\max} = \alpha_{\max}(0.9) = 0.287$ and $\alpha_{\max} = \alpha_{\max}(0.99) = 0.117$, and consider the values $\beta = \delta$ varying from 0.01 to 0.1. One sees in Fig. 11 that the retro-reflectivity ratio approaches the corresponding value $r(\alpha_{\max}, k)$ (marked by a point on the vertical axis) as β goes to 0.

The three graphs of maximum retro-reflectivity ratio versus k with fixed values of β and δ are shown in Fig. 12. The two graphs are related to the values

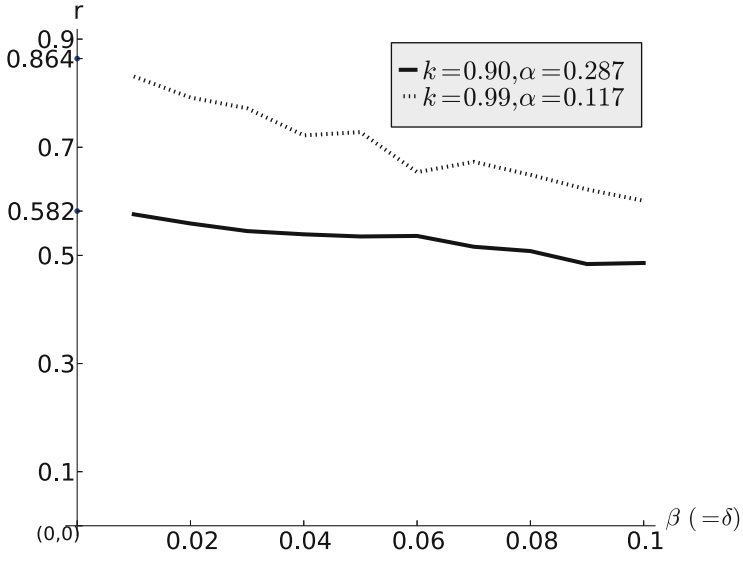


Fig. 11. The plot of the retro-reflectivity ratio *vs* $\beta (= \delta)$ for $k = 0.9$ and $k = 0.99$.

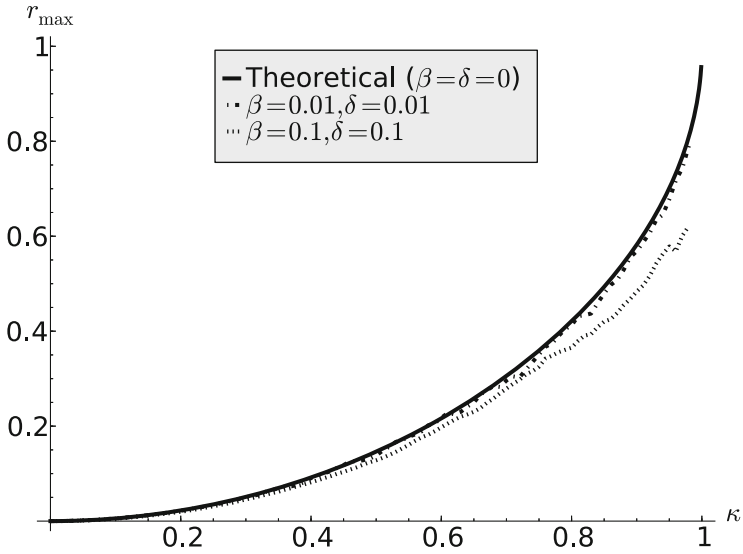


Fig. 12. The graphs of maximum retro-reflectivity ratio *vs* k in the three cases when (a) $\beta = \delta = 0.1$; (b) $\beta = \delta = 0.01$; and (c) the theoretical limiting case for $\beta = \delta = 0$.

$\beta = \delta = 0.1$ and $\beta = \delta = 0.01$, and the third graph plots the theoretical maximum value $\max_{\alpha} r(\alpha, k)$, which corresponds to the limiting case $\beta = \delta = 0$.

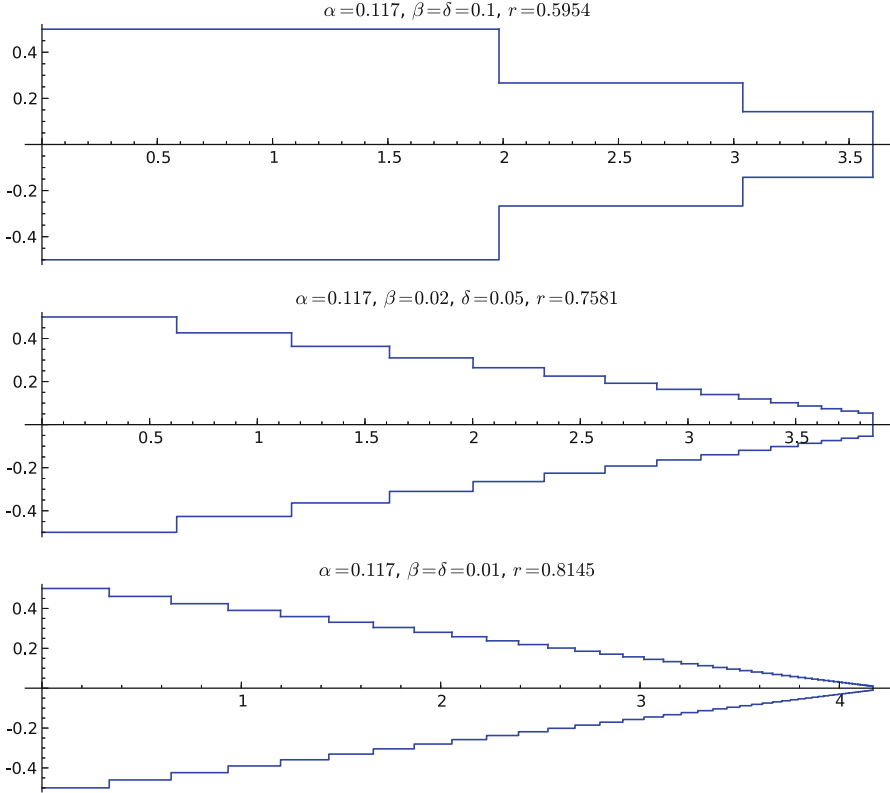


Fig. 13. Three special shapes of Notched angle with $k = 0.99$ and $\alpha = \alpha_{\max}(k) = 0.117$ and with high retro-reflectivity ratios.

Again, it is seen that the maximum retro-reflectivity approaches its theoretical limit as $\beta \rightarrow 0$, $\delta \rightarrow 0$, and is very close to this limit when $\beta = 0.01$, $\delta = 0.01$.

A numerical work has been done on finding practical shapes with retro-reflectivity ratio higher than that of the well-known shape Square corner. The reflection coefficient was taken to be $k = 0.99$. We also took $\alpha = 0.117$, the optimal angle corresponding to the value $k = 0.99$. The results are presented in Fig. 13.

There always is a tradeoff between simplicity of the shape and high retro-reflectivity. The three shapes presented in the figure have the ratios $r \approx 0.6$, 0.76 , and 0.82 , which are significantly greater than the ratio of the Square corner $k^2(\sqrt{2} - 1) \approx 0.4$. Naturally, the greater the ratio, the more complicated is the shape: in the first case one has $\beta = \delta = 0.1$, in the second case $\beta = 0.02$, $\delta = 0.05$, and in the third case $\beta = \delta = 0.01$.

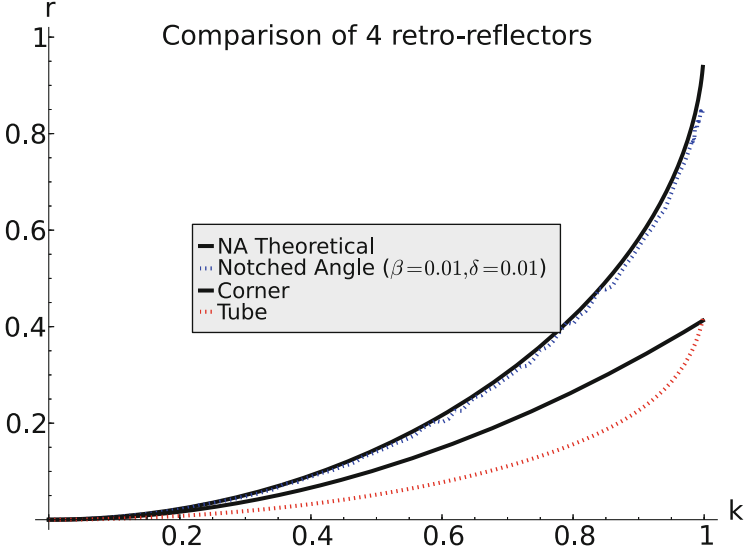


Fig. 14. The plots of the retro-reflectivity ratio *vs* *k* for the retroreflectors (a) Tube with $n = 49$, $d = 0.2$, $\varepsilon = 0.05$, (b) Notched angle with $\beta = \delta = 0.01$ and with $\alpha = \alpha_{\max}(k)$, (c) the square corner, and (d) $r(\alpha_{\max}, k)$, the retro-reflectivity ratio of Notched angle with $\beta \rightarrow 0$, $\delta \rightarrow 0$.

3 Tube and Comparison with Notched Angle

It was proved in [1,5] that there exist Tube retroreflectors with retro-reflectivity ratio arbitrarily close to 1. More precisely, suppose that the sides of the retroreflector are perfectly reflecting, $k = 1$; then we have $r(B(n, d, \varepsilon)) \xrightarrow[\varepsilon \rightarrow 0]{} 1$ for a certain family of retroreflectors with the size of small segments going to zero, $\varepsilon \rightarrow 0$, and their number going to infinity, $n = n(\varepsilon) \rightarrow \infty$, and with fixed distance d between the segments.

There are no analytical formulas for the retro-reflectivity ratio of Tube with positive values of the parameters ε , n , and d , so we did an extensive numerical simulation with ε taking the values in $\{0.01, 0.05, 0.1, 0.2\}$ and with $k < 1$, searching for the values of n and d that provide the best retro-reflectivity ratio. We found that the retro-reflectivity ratio of Tube is generally much smaller than that of Notched angle, and even of the square corner, as seen in Fig. 14. The reason is that Tube requires a huge number of light reflections. As a result, when $k < 1$, a large portion of light is absorbed, thus lowering the retro-reflectivity ratio.

In Fig. 14 the retro-reflectivity ratios of three retroreflectors are compared: (a) Tube with $n = 49$, $d = 0.2$, $\varepsilon = 0.05$; (b) Notched angle with $\beta = \delta = 0.01$ and with $\alpha = \alpha_{\max}(k)$ taken to be optimal, (c) the square corner, and (d) the function $r(\alpha, k)$ (2) with $\alpha = \alpha_{\max}(k)$ (recall that it defines the retro-reflectivity ratio in the limiting case of Notched angle with $\beta \rightarrow 0$, $\delta \rightarrow 0$).

Acknowledgements. This work was supported by Portuguese funds through CIDMA– Center for Research and Development in Mathematics and Applications and FCT – Portuguese Foundation for Science and Technology, within the project PEst-OE/ MAT/ UI4106/ 2014, as well as by the FCT research project PTDC/ MAT/ 113470/ 2009.

References

1. Bachurin, P., Khanin, K., Marklof, J., Plakhov, A.: Perfect retroreflectors and billiard dynamics. *J. Mod. Dynam.* **5**, 33–48 (2011)
2. Eaton, J.E.: On spherically symmetric lenses. *Trans. IRE Antennas Propag.* **4**, 66–71 (1952)
3. Luneburg, R.K.: *Mathematical Theory of Optics*. Brown University, Providence (1944)
4. Ma, Y.G., Ong, C.K., Tyc, T., Leonhardt, U.: An omnidirectional retroreflector based on the transmutation of dielectric singularities. *Nat. Mater.* **8**, 639–642 (2009)
5. Plakhov, A.: Mathematical retroreflectors. *Discr. Contin. Dynam. Syst.-A* **30**, 1211–1235 (2011)
6. Plakhov, A.: *Exterior Billiards: Systems With Impacts Outside Bounded Domains*, XIII, 284 pp., 108 illus. Springer, New York (2012)
7. Plakhov, A., Gouveia, P.: Problems of maximal mean resistance on the plane. *Nonlinearity* **20**, 2271–2287 (2007)
8. Tyc, T., Leonhardt, U.: Transmutation of singularities in optical instruments. *New J. Phys.* 10(115038), 8pp (2008)
9. Walker, J.: Wonders with the retroreflector. *The Amateur Scientist. Scientific American*, April 1986

Optimization in the Natural Sciences

30th Euro Mini-Conference, EmC-ONS 2014, Aveiro,

Portugal, February 5-9, 2014. Revised Selected Papers

Plakov, A.; Tchemisova, T.; Freitas, A. (Eds.)

2015, X, 207 p. 72 illus., Softcover

ISBN: 978-3-319-20351-5